Received: 16 April 2021 | Revised: 6 July 2021 | Accepted: 14 August 2021

DOI: 10.1002/suco.202100253

ARTICLE

fib CEB-FIP WILEY

Structural and economical performance of reinforced concrete frames with Dual-Phase and TempCore® steel rebars in uncorroded and corroded conditions

Silvia Caprili | **Francesca Mattei** | **Walter Salvatore**

Department of Civil and Industrial Engineering, University of Pisa, Pisa, Italy

Correspondence
Francesca Mattei, Department of Civil and Industrial Engineering, University of Pisa, Largo Lucio Lazzarino 1, 56122 Pisa, Italy.
Email: francesca.mattei@ing.unipi.it

Funding information
Research Fund for Coal and Steel, Grant/Award Number: RFSR-CT-2015-00023

Abstract

In the last decades, the need to develop new enhanced typologies of steel reinforcement bars with improved ductility and durability performance in presence of aggressive environmental conditions progressively increased due to the negative consequences that corrosion showed on the structural capacity of reinforced concrete (RC) buildings. Within the recently concluded NEWREBAR research project, a new reinforcing steel grade with Dual-Phase (DP) microstructure and selected low-carbon content chemical composition (kept in the range of the actual European production) was developed, produced, and tested even in presence of accelerated induced corrosion. To understand the impact of the adoption of DP rebars in RC structures, case study buildings were designed, modeled, and analyzed using the new grade and compared to traditional buildings using TempCore® rebars. In the present work, the results of a techno-economic analysis performed on both DP and TempCore® RC buildings through the evaluation of the expected annual loss (EAL) index is presented for a residential five-storeys case-study building, assessing the benefit introduced by adopting the proposed new reinforcing grade even in presence of corrosion.

KEYWORDS

corrosion, Dual-Phase, expected annual loss, incremental dynamic analysis, reinforced concrete, TempCore®

1 | INTRODUCTION

Durability problems affecting reinforced concrete (RC) constructions in the last years pushed research activities in the field of developing, producing, and applying new enhanced typologies of reinforcing steels characterized by improved performance even after corrosion attack, especially in terms of deformation capacity. As known, corrosion is responsible for the decrease of the bearing capacity

Abbreviations: DP, Dual Phase; EAL, expected annual loss; RC, reinforced concrete.

Discussion on this paper must be submitted within two months of the print publication. The discussion will then be published in print, along with the authors' closure, if any, approximately nine months after the print publication.

of RC buildings (e.g., References 1–6). Main consequences of corrosion attack consist in the cracking and spalling of the concrete cover, the loss of bond between rebars and concrete and the increasing reduction of the rebars' cross section. Two main problems, in particular, may affect reinforcing bars, depending on the corrosion attack: in presence of uniform corrosion a wide decrease of the cross-section area can be observed, with a resulting lower amount of steel per section; pitting/localized phenomena, on the other hand, are associated to the reduction of the deformation capacity, whose residual values can drop even below the threshold imposed by current standards for (new) RC constructions (EN1998-1:2005[7]; D.M.17/01/2005). The above-mentioned phenomena were widely observed in TempCore® bars, commonly adopted for constructions thanks to the combination of good mechanical properties and moderate production costs. The TempCore® external martensitic layer, even if providing good strength, exposes rebars to relevant durability problems related to the C-content[8–11]: the higher is the C-content, the higher is the tendency to corrosion. In TempCore® rebars, the decrease of the mechanical performance can become relevant[12] having impact on the overall RC building behavior even altering what imposed following the capacity design philosophy and the preselection of dissipative regions. Besides the protection measures suggested by Eurocodes and other standards (EN1992-1-1:2005[13]; EN 206–1:2006[14]) that increase concrete strength class or concrete cover thickness to limit corrosion effects, prevention strategies can be developed by introducing enhanced materials less sensitive to durability problems.

It was following this idea that during the last years Dual-Phase (DP) rebars were deeply investigated[15,16]: their typical microstructure, where martensite and ferrite coexist in the same matrix, highly reduces the sensitivity to corrosion phenomena providing, in the meanwhile, adequate strength and deformation capacity. In the framework of the European RFCS project NEWREBAR *"New Dual-Phase steel reinforcing bars for enhancing capacity and durability of anti-seismic moment resisting frames"* (2015–2019), new enhanced typologies of reinforcing bars with DP microstructure were developed, produced, characterized, and applied to constructions, highlighting the improvement given in terms of structural and economic convenience.[17–22] In the present work, the techno-economic impact of adopting DP grades in RC constructions as alternative to traditional TempCore® is analyzed through the evaluation of the expected annual loss (EAL) index for a typical residential case-study building, in reference, and corroded conditions. The aim of the adopted procedure is, besides highlighting the "performance" benefit related to the higher durability of DP rebars, showing that costs connected to the introduction of a new product on the reinforcement market can be justified and sustained if kept below a reasonable threshold.

2 | DUAL-PHASE STEEL REBARS AND TEMPCORE®

The improved durability performance of DP rebars is the direct consequence of the particular microstructure not presenting the external-hard martensitic layer, main responsible for corrosion in TempCore®. The DP microstructure is achieved through a particular production process actually used only for flat or sheet products, making DP steels widely used in the automotive sector but strongly limited for civil structural and infrastructural applications. The production process (by hot-rolling route or by the application of a post intercritical quenching treatment[17]) leads to an undefined yielding stress–strain law with mechanical parameters—mainly in terms of hardening ratio—not always aligned with what required by actual standards for constructions (EN1998-1:2005[7]): if we look to common DP grades (like DP800 or DP1000) the ratio R_m/R_e can be beyond the value of 1.35, upper limitation for ductility class "C" rebars.

Tensile tests were performed to fully characterize the mechanical properties of the new proposed DP grades; in particular, as presented in Caprili et al.,[22] two different chemical compositions with slightly different carbon content were adopted, respectively indicated as DPF and DPD (C-content, respectively, equal to 0.160% and 0.233%, this last one comparable with what normally presented for a TempCore® B450C grade). The typical experimental stress–strain curves are presented in Figure 1. The whole data set of experimental tests can be found in Caprili et al.[17]; Table 1 summarizes the average values of the mechanical properties for the different steel grades in reference condition.

Recent studies in the current scientific literature proved that the parameters mostly affected by corrosion are the ones connected to the deformation capacity, that is, the elongation to maximum load (A_{gt}), the hardening ratio $\left(R_m/R_e\right)$ and, eventually, the deformation at failure (A_5). The impact on material ductility is of course reflected at section and element level, with reduction of the capacity expressed in terms of curvature or rotation.

The enhanced performance of DP rebars respect to TempCore® B450C was proved by comparing the residual values of the mechanical parameters achieved for the same corrosion entity, expressed in terms of mass loss (ML) referred to the exposed length. As widely presented in Caprili et al.,[17] TempCore® B450C highlighted higher reduction of the mechanical properties: considering ML of about the 5%, the average residual deformation capacity (ResA_{gt}) was respectively the 54% and the 70% of the uncorroded value for B450C and DPF steel reinforcing bars. Translating into numbers and considering the reference values presented in Table 1, this means that for initial A_{gt} values, respectively, equal to 13.9% and 15.1% for DPF and B450C rebars, residual ResA_{gt} up to 9.7% and 8.5% would be observed for ML equal to 5.0%.

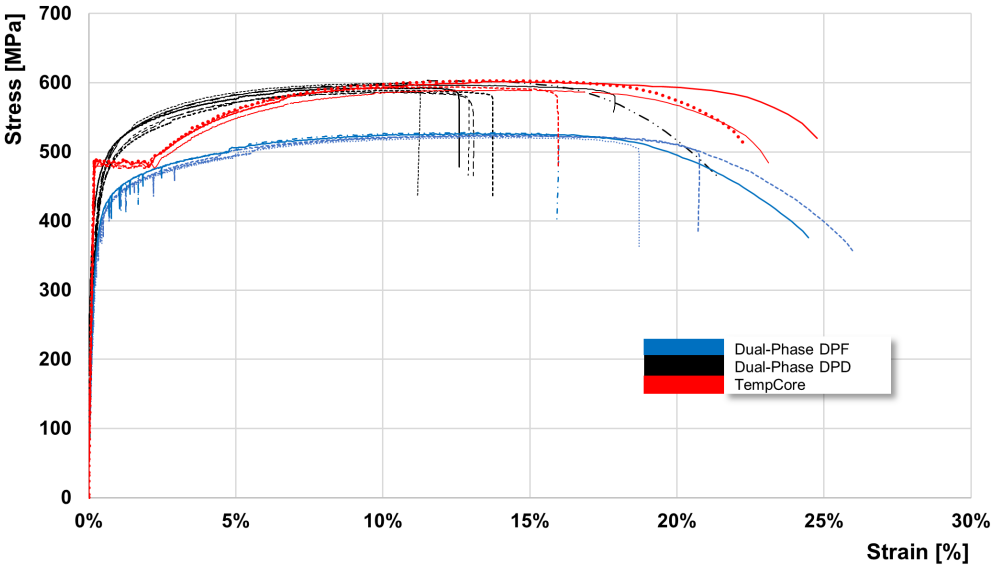

FIGURE 1 Experimental stress–strain curves for the different steel reinforcing bars considered: DPF, DPD, and B450C

TABLE 1 Average results of mechanical properties from tensile tests (reference condition) for DP and TempCore® steel grades, being R_m or $R_{p,02}$ the yielding strength for defined or undefined yielding rebars, R_m the ultimate tensile strength, A_{gt} and A_5, respectively, the elongation to maximum load and the ultimate elongation and Z the necking

Grade	R_e or $R_{p,02}$ (MPa)	R_m (MPa)	R_m/R_e (−)	A_{gt} (%)	A_5 (%)	Z (%)
DPF	403.6	525.1	1.3	13.90%	31.50%	51.1
B450C	485.7	594.8	1.22	15.70%	26.70%	42.3

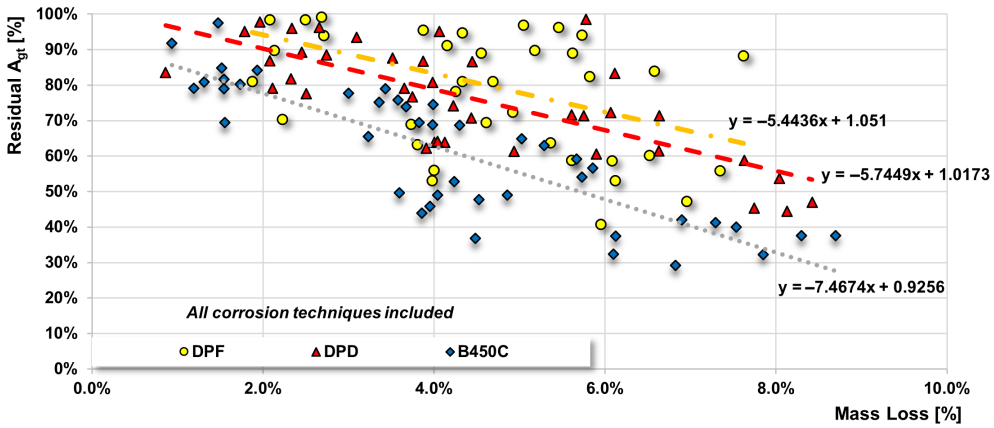

FIGURE 2 Residual A_{gt} in relation to achieved values of mass loss (ML) and simplified linear tendency (data provided in Caprili et al.[18])

Figure 2 shows the decrease of A_{gt} in relation to the increase of mass loss (ML—corrosion entity) and the linear simplification of the trend of residual values of A_{gt} for increasing ML. The diagram is derived from the experimental data presented in Caprili et al.[17]

3 | DESIGN, MODELING, AND ANALYSIS OF RC-DP AND RC-TEMPCORE® BUILDINGS

3.1 | Design of case studies

RC case study buildings were designed using both DP and TempCore® B450C rebars. The selected building is a residential moment resisting frame (MRF) structure with a rectangular shape of dimensions 60 × 14 m^2 (Figure 3), five floors and beams with length equal to 4.0 and 6.0 m; the interstorey height is up to 2.50 m (first level—garage) and 3.0 m (other levels). The design was performed according to EN1998-1:2005[7] and D.M.17/01/2018[23] following the capacity design approach. The same indications adopted for ordinary RC buildings were followed, even concerning structural details of sections and elements; this choice was the direct consequence of what observed in References 19 and 20 about the reliability of adopting the capacity design rules even for DP grades, achieving the expected performance of RC substructures.

Vertical loads were defined in relation to the typology of structural and not structural used components (storey

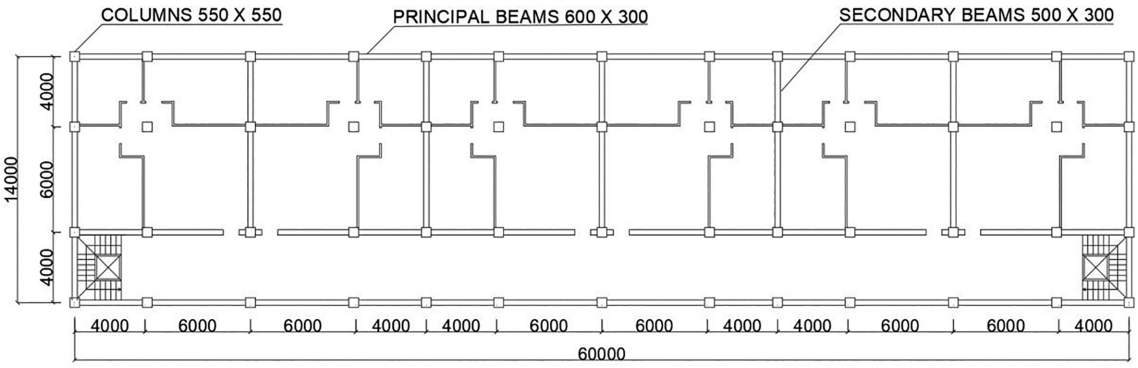

FIGURE 3 Typical storey plan for the residential building

slab, roof, internal and external infills, equipment, etc.); Eurocode 1 was adopted for live loads. Predalle H24-i50 system, characterized by a total height of 24 cm and spacing between longitudinal joists equal to 50 cm were adopted for storey slabs, resulting in a permanent structural load (G_1) equal to 3.35 kN/m^2. Concrete slabs, floor, and internal infills were then considered, resulting in a permanent not structural load (G_2) up to 2.75 kN/m^2; the live load acting on roof was fixed equal to 0.50 kN/m^2 while for intermediate floors Q_k was assumed up to 2.0 kN/m^2. Concerning materials, concrete class C25/30 and exposure class XS2 (EN1992-1-1:2005[13]) was considered; for rebars, DP DPF[22] and TempCore® B450C were employed, whose characteristics are summarized in Table 1.

The selected case-study building was located in Avezzano (Abruzzo, Italy); the seismic action was evaluated according to the national prescriptions (D.M.17/01/2018[23]) assuming soil category B, nominal life (V_N) equal to 50 years and Use Class II. A behavior factor equal to 5.85 was considered (corresponding to structures designed for high ductility class). Response spectrum Type 1 (EN1998-1:2005[7]) was adopted, being possible earthquakes with magnitude higher than 5.5.

As a general comment concerning differences encountered by the two buildings, being the design yielding strength of reinforcing steel DPF (R_e), the 28% lower than the one associated to B450C rebars (403.6 MPa vs. 485.7 MPa), main variations concerned the longitudinal and transversal reinforcement amounts. The gross sections of beams and columns were kept constant, otherwise varying reinforcing ratio in relation to structural needs. Table 2 briefly schematizes the layout of RC-DPF and RC-B450C typical beams' and columns' sections, highlighting differences in the rebars' total amount. As visible, the longitudinal and transversal reinforcement ratios were, respectively, the 20% and the 28% higher in case of DP adoption for columns and 28% and 20% in beams.

3.2 | Nonlinear modeling

The structural performance was assessed through the execution of nonlinear static and dynamic analyses, using ground motions selected as presented in the following paragraph. Case study buildings were modeled and analyzed in reference and corroded conditions. Two-dimensional frame models with lumped plastic hinges were elaborated for each of the two main directions using the OpenSees® software.[24] The modeling of the nonlinear behavior was limited to those portions where relevant cracks occurred according to the experimental evidence, as discussed in Caprili et al.[19,20] keeping elastic all the other parts not involved in plastic deformations. To describe the nonlinear behavior of plastic hinges a specific nonlinear mechanical model was elaborated by the authors, where the main features of the RC section are represented along the plastic hinge length through truss elements, similarly to what performed through a fiber-section approach. The mechanical model was calibrated in its components using the results of the experimental campaign presented in Caprili et al.[19,20] and therefore adopted for different sections of elements. Moment–rotation (M–θ) relationships were then directly derived from the mechanical model without requiring the adoption of consolidated equations valid, perhaps, mainly for ordinary reinforcing steels with defined yielding plateau. A further multilinear schematization was besides introduced by defining four relevant points associated to first cracking (CR), yielding (Y), maximum bending action (M), and ultimate condition (U), see Figure 4.

For the modeling of rebars, the Pinching4 Model from OpenSees® library was used, while Mander law[25] was adopted for concrete. Bond-slip effect was introduced by adopting the simplified model proposed by Caprili et al.[21] as direct modification of the constitutive law for steel rebars, starting from the well-validated assumptions presented in Braga et al.[26,27] and D'Amato et al.[28]

TABLE 2 Total amount of longitudinal (r) reinforcements in RC-DPF and RC-B450C typical sections

				RC-DPF				RC-B450C				% Variation	
ID element		H [m]	B [m]	Rebars	ρ	Stirrups	ω	Rebars	ρ	Stirrups	ω	Δρ	Δω
Columns	P1	0.55	0.55	16ϕ22	2.0%	8ϕ8/80	24%	16ϕ20	1.6%	8ϕ8/120	19%	21%	28%
	P2	0.50	0.50	16ϕ22	2.4%	8ϕ8/80	27%	16ϕ20	2.0%	8ϕ8/120	21%	21%	28%
	P3	0.45	0.45	16ϕ22	3.0%	8ϕ8/80	30%	16ϕ20	2.4%	8ϕ8/120	24%	21%	28%
Beams	A	0.60	0.30	4ϕ18 + 4ϕ16	1.0%	4ϕ10/120	15%	4ϕ16 + 4ϕ14	0.8%	4ϕ10/100	19%	28%	18%
	B	0.60	0.30	4ϕ18 + 2ϕ16	0.8%	4ϕ10/120	15%	4ϕ16 + 2ϕ14	0.6%	4ϕ10/100	19%	28%	18%
	C	0.60	0.30	4ϕ18 + 3ϕ16	0.9%	4ϕ10/120	15%	4ϕ16 + 3ϕ14	0.7%	4ϕ10/100	19%	28%	18%

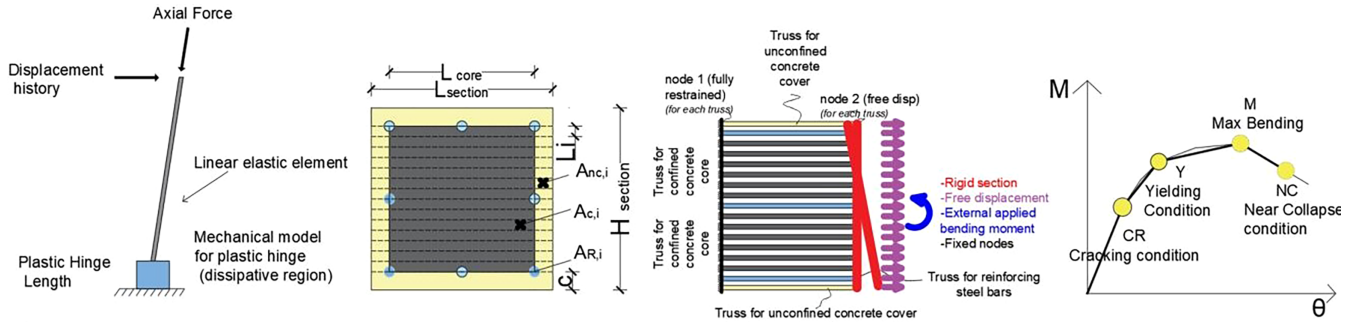

FIGURE 4 Schematization adopted for the mechanical model and simplified moment–rotation (M–θ) law for plastic hinges in frame models

In corroded conditions, the modification of the elements' capacity (and therefore of the M–θ relationship) caused by to the decrease of the mechanical performance of materials was introduced. Steel properties' modification as well as the cross-section reduction were included in the model, otherwise neglecting concrete degradation and bond strength deterioration, assuming—basing on the experimental evidence—that for values of ML lower than 5% not a strong relevance is owned by such phenomena.

Experimental data presented in Caprili et al.[22] and Caprili et al.[17] were used for the calibration of the constitutive laws in corroded conditions. Considering design class XS2, ML of about 5% was evaluated for a high corrosion rate in combination with a sufficient concrete cover thickness after approximately 45 years. Correlations between mechanical performance and ML, based on common formulas proposed by the current scientific literature, allowed to evaluate the decrease of deformation, strength and the cross-section reduction. The average value for Res(A_{gt}) for DPF was the 70% of reference ones while, in case of TempCore® B450C, the decrease of the deformation capacity was up to the 54%. Constitutive relationships of steel rebars were consequently derived and introduced in the models: from the laws, the decrease of the deformation capacity of rebars due to corrosion is evident (Figure 5a**)** as well as the reduction of strength and deformation of concrete due to the modification of the confinement ratio (Figure 5b).

Figure 6a,bshows, respectively, for a RC section with B450C and DPF rebars in reference and corroded conditions (column section P1, see Table 2), the continuous moment/rotation relationships derived from the adoption of the mechanical model and the corresponding simplification using relevant points.

3.3 | Seismic input selection

For the execution of nonlinear incremental dynamic analyses (IDA)[29], accelerograms were selected basing on the dynamic features of the structure; conditional spectrum as a target spectrum for ground motion (GM) selection was used (Morelli et al.[30]) and defined basing on SHARE seismic hazard[31,32] (Šebenik and Dolšek,[33]), where the mean magnitude and mean distance were obtained from disaggregation of spectral acceleration corresponding to a return period of 2475 years, the first vibration period ($T_1 = 0.581$s) of and location of a structure. Ten GMs of events with magnitude in the range 4.5–7.0 and source-to-site distance between 5 and 50 km were selected; the average response spectrum associated to selected GMs was in good agreement with the design spectrum adopted for case study buildings (Figure 7).

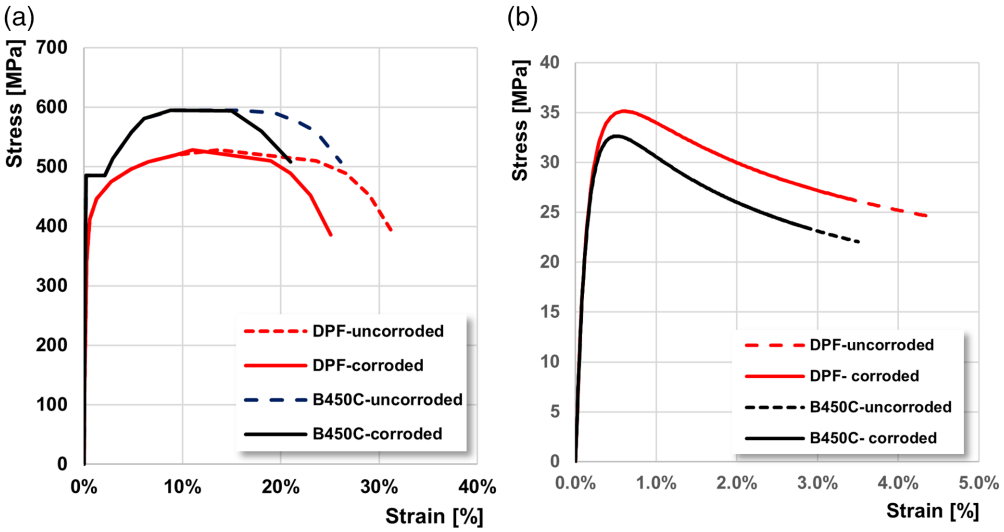

FIGURE 5 (a) Constitutive laws for rebars in reference and corroded conditions used in the model. (b) Constitutive laws for confined concrete in reference and corroded conditions used in the model

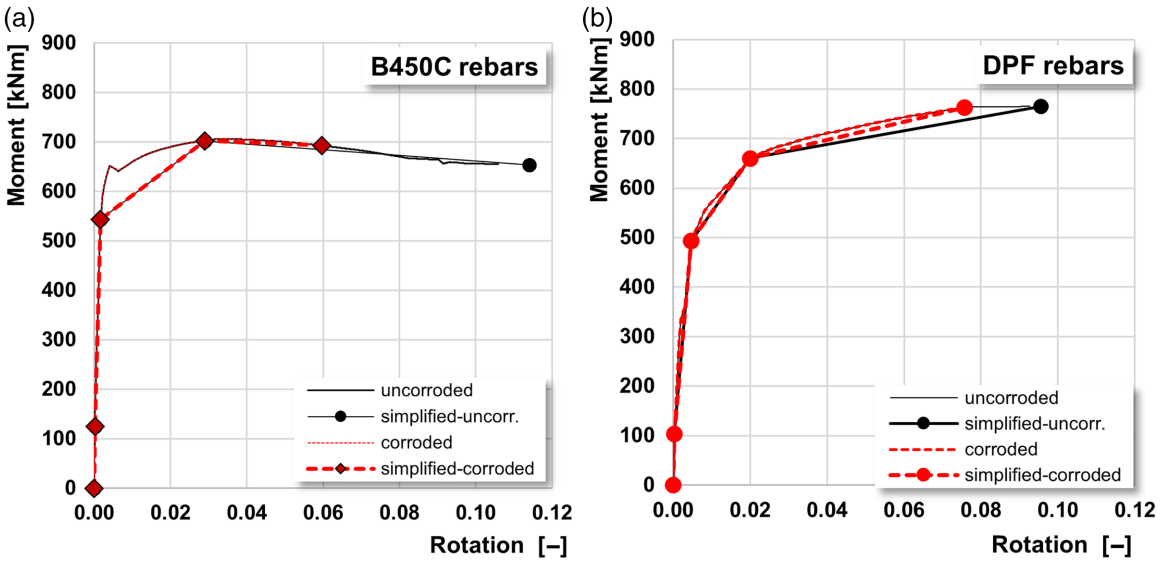

FIGURE 6 (a) Moment–rotation laws for a typical reinforced concrete (RC) element with TempCore® steel in reference and corroded conditions. (b) Moment–rotation laws for a typical RC element with DPF steel in reference and corroded conditions

3.4 | Structural performance of case study buildings

The structural assessment was performed by comparing the seismic demand coming from nonlinear static and dynamic analyses (i.e., rotations for ductile mechanisms and shear force for brittle ones) with the corresponding elements' capacity, that is, yielding and ultimate rotations coming from moment–rotation laws previously described and shear resulting from the application of EN1998-3:2005[7] rules.

3.4.1 | Selection of collapse criteria

Criteria adopted for assessing the reaching of relevant limit states (immediate occupancy—IO; damage limitation—DL; life safety—LS; near collapse—NC) are summarized in Table 3.

For sake of clarity, the determination of the engineering demand parameters (EDP) associated to relevant limit states has, actually, not a unique definition (Terrenzi et al.[34]), being indications provided by EN1998-3:2005[7] (and, similarly D.M.17/01/2018[23]) for collapse EDP fixed for existing buildings but not for new ones. For existing structures, specific values of chord rotation in beams or columns, that is, element-based criteria, are given. FEMA 356, on the contrary, proposes global EDP such as interstorey drift ratio (IDR) to define ultimate and serviceability conditions, with values between 1.0% (IO) and 4.0% (NC). Italian D.M.17/01/2018[23] even provides criteria related to IDR for new buildings at DL (i.e., $IDR_{DL} = 0.5\%$) and IO limit states (i.e., $IDR_{IO} = 2/3\ IDR_{DL} = 0.333\%$). Criteria provided by EN1998-3:2005[7] were,

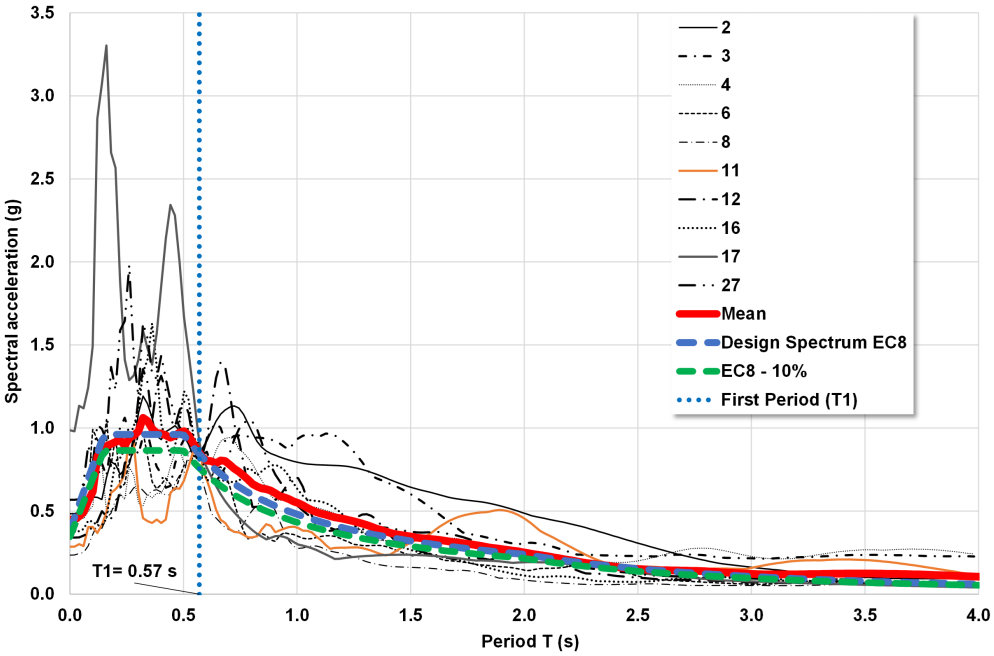

FIGURE 7 Response spectra associated to selected ground motions (GMs) and comparison with the design spectrum for case studies

TABLE 3 Criteria for the evaluation of PGA capacity for different limit states

Limit state		Criteria for PGA_c determination
IO	Immediate occupancy	$2/3\theta_y$
DL	Damage limitation	θ_y
LS	Life safety	$3/4\theta_u$
NC	Near collapse	θ_u

Abbreviations: DL, damage limitation; IO, immediate occupancy; LS, life safety; NC, near collapse.

therefore, used for NC (i.e., θ_u), LS (i.e., $¾\theta_u$), and DL (i.e., f θ_y), extending the element-based concept normally used for existing structures to new ones; for IO, the achieving of $⅔\theta_y$ was used. Table 3 shows what has been adopted in the present research work.

3.4.2 | Results of structural assessment

Results of nonlinear analyses highlighted a ductile collapse modality caused by the achieving of the ultimate chord rotation in the first element, neglecting—thanks to the capacity design approach—brittle/shear failures.

The differences in terms of structural response, evaluated from capacity curves and IDR along the height, between the RC-DPF and RC-B450C case studies were negligible (Figure 8a,b). Being the yielding strength of DPF rebars lower respect to TempCore®, and therefore being higher their total amount of longitudinal rebars, a slight increase of the maximum base shear was observed for RC-DPF, with difference in general not higher than 7%.

IDA results allow to draft additional considerations (Figure 9a,b). The RC-B450C building showed an initial stiffness higher than the one provided by the RC-DPF one (Figure 10a); the same behavior was visible, perhaps, even at material level: this means that the yielding chord rotation (θ_y) is achieved for lower values of PGA if TempCore® is used in the design instead of DPF. The reaching of the ultimate chord rotation (θ_u) in the first element was used as global collapse criterion and, in this case, the structural performance of buildings was strictly dependent on the reinforcing steel material adopted. To better explain, for low axial load (or even null such as in beams) being A_{gt} higher for B450C respect to DPF (Figure 1), the ultimate curvature χ_u and therefore the ultimate rotation θ_u was higher for RC-B450C elements; on the contrary, in presence of relevant axial loads (e.g., columns), the values of χ_u and θ_u depended on the ultimate concrete strain ε_{cu}, normally higher in case of DPF elements being dependent on ultimate deformation of the rebars and on confinement ratio.

Considering the corroded condition and the relative modification of the mechanical properties of rebars, the PGA levels activating DL (θ_y) were almost unchanged while the ones related to NC (θ_u) were higher in case of RC-DPF building: this was due to the fact that, for the same ML, values of A_{gt}—influencing the ultimate performance—were lowered from 13.9% to 11.07% and from 15.7% to 8.67%, respectively, in case of DPF and TempCore® B450C.

Differences between RC-DPF and RC-B450C in terms of base shear (V_{max}) and top displacement (d_{max}) corresponding

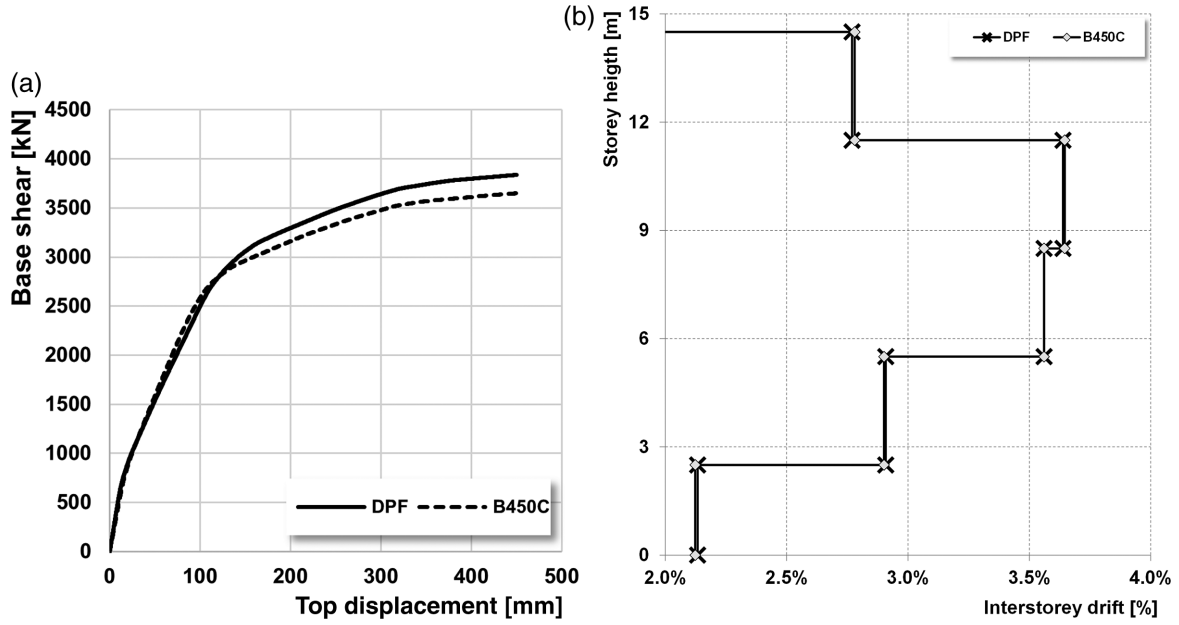

FIGURE 8 (a) Comparison in terms of capacity curves for case study building designed with DPF and B450C (pushover). (b) Comparison in terms of IDR for case study building designed with DPF and B450C (pushover)

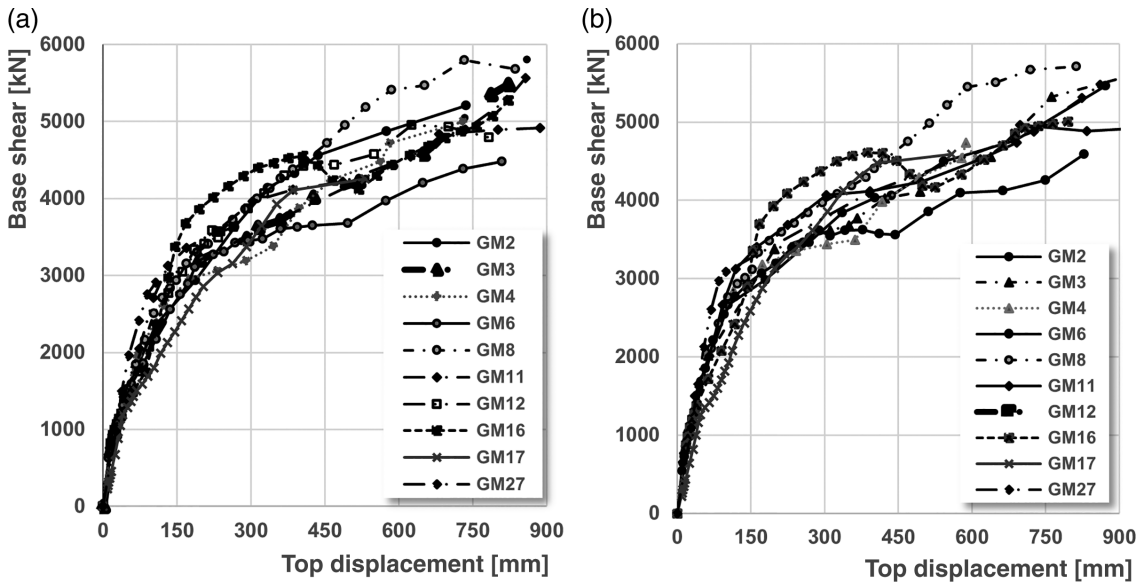

FIGURE 9 (a) Base shear/top displacement curves from IDA for RC-DPF case study—reference condition. (b) Base shear/top displacement curves from IDA for RC-B450C case study—reference condition

to the first achievement of θ_u (PGA values are indicated too) are presented in Table 4 and in Table 5 for the reference and corroded conditions. The average values of V_{max} and d_{max} achieved for the 10 considered accelerograms were higher, in both the sound and corroded condition; it shall be noted that this is partially a consequence of the higher amount of longitudinal/transversal reinforcement coming from the design performed with slightly lower values of the design yield strength and, partially, due to the corrosion effects, as showed even in the next paragraphs.

4 | TECHNO-ECONOMIC ANALYSIS OF RC-DP BUILDINGS

4.1 | Expected annual loss index

The impact of DP steel grade on the structural performance of RC buildings was assessed through the EAL index,[35] a parameter joining together the structural response and the economic impact to evaluate how DP influence RC construction performance with reference to traditional TempCore® rebars.

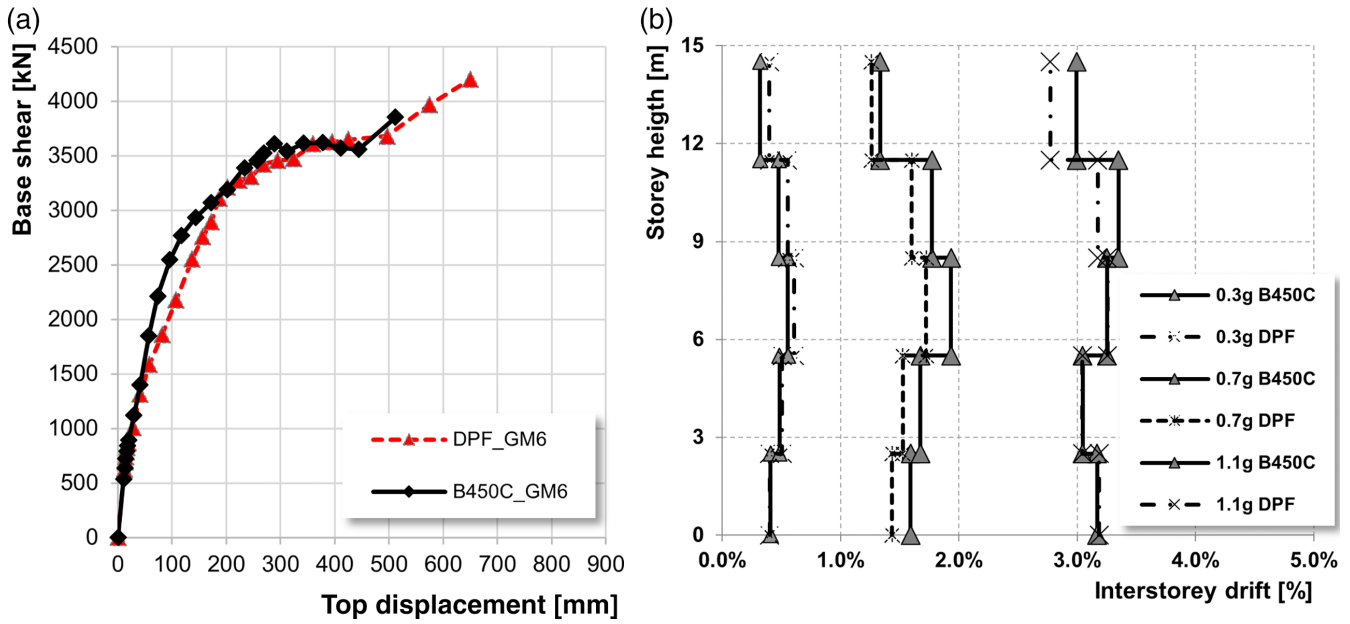

FIGURE 10 (a) Base shear/top displacement for GM6 in corroded conditions. (b) IDR for GM6 in corroded conditions

TABLE 4 Base shear and top displacement values at first ultimate chord rotation for reference conditions

	Reference condition										
RC-DPF	**GM2**	**GM3**	**GM4**	**GM6**	**GM8**	**GM11**	**GM12**	**GM16**	**GM17**	**GM27**	**Average**
V_{max} [kN]	5209	6055	4996	4451	5680	4913	4795	5477	4251	5563	**5139**
d_{max} [mm]	737	888	729	889	836	886	782	855	532	857	**799**
PGA [g]	1.00	1.10	1.20	1.60	1.70	0.80	1.60	1.90	1.70	2.10	**1.47**
RC-B450C	**GM2**	**GM3**	**GM4**	**GM6**	**GM8**	**GM11**	**GM12**	**GM16**	**GM17**	**GM27**	**Average**
V_{max} [kN]	5460	5569	4527	4590	5707	4913	4962	5002	4585	5479	**5079**
d_{max} [mm]	872	908	608	829	813	915	772	796	558	860	**793**
PGA [g]	1.00	1.00	1.20	1.50	1.70	0.80	1.60	1.80	1.90	2.10	**1.46**

TABLE 5 Base shear and top displacement at first ultimate chord rotation for corroded conditions

	Corroded condition										
RC-DPF	**GM2**	**GM3**	**GM4**	**GM6**	**GM8**	**GM11**	**GM12**	**GM16**	**GM17**	**GM27**	**Average**
V_{max} [kN]	4561	4577	4722	4200	5468	4541	4949	4788	3924	4894	**4663**
d_{max} [mm]	436	650	582	649	653	624	626	694	352	736	**600**
PGA [g]	0.80	0.80	1.10	1.30	1.50	0.60	1.40	1.40	1.50	1.80	**1.22**
RC-B450C	**GM2**	**GM3**	**GM4**	**GM6**	**GM8**	**GM11**	**GM12**	**GM16**	**GM17**	**GM27**	**Average**
V_{max} [kN]	4059	4111	4289	3854	5217	4232	4609	4327	3615	4874	**4319**
d_{max} [mm]	436	495	492	512	549	497	460	578	275	725	**502**
PGA [g]	0.7	0.7	0.9	1.1	1.3	0.55	1.2	1.1	1.4	1.8	**1.08**

Peak ground acceleration (PGA) values activating relevant limit states were used to account for the structural performance, while costs related to damages' repair—expressed in terms of percentage of the reconstruction cost (%CR)—were used for the economic assessment.

Equation (1) was used to achieve the annual exceedance probability (λ) for the different limit states through corresponding return periods $T_{R,C}$ calculation according Equation (2), being $\eta = 1/0.41$ as shown in Equation (3), being the subscripts *"c"* and *"d"* referred to capacity and seismic demand.

$$\lambda_i = 1/T_{R,c} \quad (1)$$

$$T_{R,c} = T_{R,d} \cdot (\mathrm{PGA}_c/\mathrm{PGA}_D)^{\eta} \quad (2)$$

$$\alpha = (PGA_C/\mathrm{PGA}_D) \cong (T_{R,C}/T_{R.D})^{\eta} \quad (3)$$

The EAL index was therefore evaluated using Equation (4) introducing the %CR associated to a specific limit state, whose values were usually fixed according to specific evaluations.

$$\mathrm{EAL} = \sum_{i=2}^{5} [\lambda(\mathrm{LS}_i) - \lambda(\mathrm{LS}_{i-1})] \cdot \frac{[\mathrm{CR}(\mathrm{LS_i}) + \mathrm{CR}(\mathrm{LS}_{i-1})]}{2} + \lambda(NC) \cdot \mathrm{CR}(\mathrm{SLR}) \quad (4)$$

It is overall accepted that LS condition is assumed for return period of the seismic event higher than the ones associated to the achievement of serviceability conditions (both DL and IO). This means that in case IO or DL were reached for $T_{R,C}$ lower than the ones associated to LS, the following assumptions would be made: $T_{R,c}(\mathrm{IO}) = \min(T_{R,c}(\mathrm{IO}); T_{R,c}(\mathrm{LS}))$ and $T_{R,c}(\mathrm{DL}) = \min(T_{R,c}(\mathrm{DL}); T_{R,c}(\mathrm{LS}))$.

In addition to IO, DL, LS, and NC two "conventional" limit states were introduced, namely, SLR (Limit State of Reconstruction) and SLID (Limit State of Initial nonstructural Damage), respectively, associated to the 100% and 0% of CR.

A repartition of %CR between structural and nonstructural components was made assuming—for ordinary RC structures 25%CR for structural elements and 75%CR for nonstructural elements. These values are commonly adopted for RC constructions with traditional reinforcing steels (FEMA E-74, Italian D.M. 65/2017[36]).

To account for the introduction of DP rebars in RC constructions, a modification of the values of %CR was introduced, considering the higher costs related to DP rebars' production. As already presented in Caprili et al.,[18] the higher %CR for RC-DP structures depends on the higher amount of DP rebars in RC structures (the lower design yielding strength as already presented in the design leads to higher reinforcement ratios) an on the higher production cost. This last one, according to the results of the industrial feasibility analysis[18] around the 5%—including both the modifications required by the industrial plant and the modification needed for production in terms of chemical components, and so forth. Considering, besides, the increase of the longitudinal and transversal reinforcement ratios already presented in the design phase, it was assessed that the overall increase of the %CR for RC-DPF construction respect to RC-B450C was around the 7.5%, leading to the values presented in Table 6 to modify the %CR for EAL evaluation.

TABLE 6 Modification of the %CR for RC-DP constructions

	RC-B450C	Splitting %CR		RC-DP
Limit state	%CR	Nonstructural components	Structural components	%CR
SLR	100%	75%	25%	101.9%
NC	80%	60%	20%	81.5%
LS	50%	38%	13%	50.9%
DL	15%	11%	4%	15.3%
IO	7%	5%	2%	7.1%
SLID	0%	0%	0%	0.0%

Abbreviations: CR, reconstruction cost; DL, damage limitation; IO, immediate occupancy; LS, life safety; NC, near collapse.

TABLE 7 PGA and T_R demand and capacity values for case study buildings, reference, and corroded conditions

			Reference condition				Corroded condition			
			RC-DPF		RC-B450C		RC-DPF		RC-B450C	
Limit state	PGA_D [g]	$T_{R,D}$ [years]	PGA [g] Av.	$T_{R,C}$ [years] Av.	PGA [g] Av.	$T_{R,C}$ [years] Av.	PGA [g] Av.	$T_{R,C}$ [years] Av.	PGA [g] Av.	$T_{R,C}$ [years] Av.
IO	0.089	30	0.19	183	0.15	101	0.19	183	0.15	101
DL	0.117	50	0.28	420	0.22	233	0.28	420	0.22	233
LS	0.29	475	1.1	12,656	1.1	12,447	0.92	8032	0.81	5899
NC	0.37	975	1.47	27,471	1.46	27,017	1.22	17,435	1.08	12,805

Abbreviations: CR, reconstruction cost; DL, damage limitation; IO, immediate occupancy; LS, life safety; NC, near collapse.

TABLE 8 EAL values in reference and corroded conditions for RC-DPF and RC-B450C buildings

	RC-DPF			RC-B450C		
Limit state	CR (%)	Reference λi	Corroded λi	CR (%)	Reference λi	Corroded λi
SLR	101.89%	0.00%	0.00%	100%	0.00%	0.000%
NC	81.51%	0.004%	0.006%	80%	0.004%	0.008%
LS	50.94%	0.008%	0.012%	50%	0.008%	0.017%
DL	15.28%	0.240%	0.240%	15%	0.429%	0.429%
IO	7.13%	0.550%	0.550%	7%	0.985%	0.985%
SLID	0.00%	10.00%	10.00%	0%	10.000%	10.000%
	EAL_{DPF}	*0.454%*	*0.457%*	EAL_{B450C}	*0.520%*	*0.524%*

Abbreviations: CR, reconstruction cost; DL, damage limitation; EAL, expected annual loss; IO, immediate occupancy; LS, life safety; NC, near collapse.

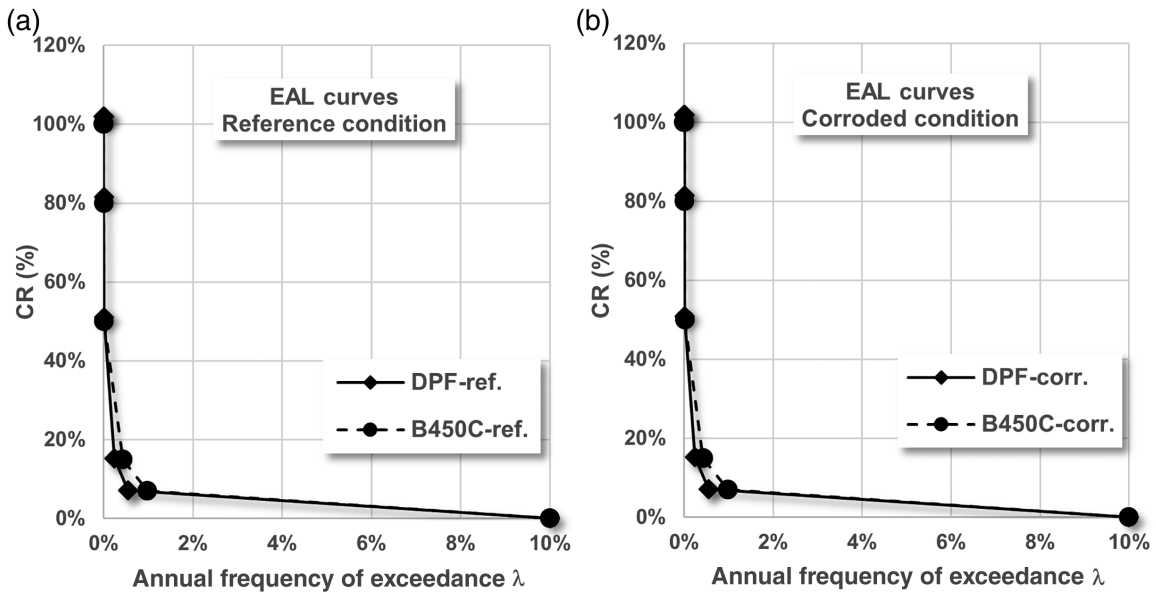

FIGURE 11 (a) EAL curves in reference conditions for the RC-DPF and RC-B450C residential buildings. (b) EAL curves in corroded conditions for the RC-DPF and RC-B450C residential buildings

4.2 | Results of EAL analysis for case studies

The capacity (average $PGA_{,C}$ and related $T_{R,C}$) for different limit states coming from the 10 selected GMs are presented in Table 7 in reference and corroded conditions; couples of values to obtain EAL curves (λ_i;CR_i) are summarized in Table 8.

As visible, PGA values activating LS condition, for all considered time histories, were lower in case of RC-B450C than in RC-DPF building; NC condition (achievement of θ_u) was achieved almost for the same level of seismic action in both the two considered case studies. This last consideration is directly related to the design approach: being the case studies designed according to the capacity design rules, the first θ_u was achieved in beams (i.e., elements only in flexure) and directly influenced by the A_{gt} value, being this last higher for TempCore® B450C. Similar NC activation levels were, otherwise, observed in relation to the higher amount of rebars adopted in the design and to the slightly higher capacity of beam elements in case of RC-DPF building respect to RC-B450C one. The presence of corrosion leaded, in general, to the reduction of PGA values activating relevant criteria: in case of RC-B450C building PGA values activating NC shifted from 1.46 g to 1.08 g, while for RC-DPF variations were lower, decreasing from 1.47 g to 1.22 g, and this was directly related to the material performance.

Looking at EAL values (Figure 11a,b, Table 8), RC-DPF and RC-B450C showed average EAL values

respectively equal to 0.45% and 0.52%, always resulting in buildings in class A (as expected for new constructions) highlighting, besides, the better performance of DP structures owing a lower value of EAL. Being EAL the area under the curve RC%-λ, its value depends on the PGA levels achieved by the structure, in particular for IO, DL, and LS limit states that weigh on the EAL calculation: these values were higher for RC-DP construction respect to RC-B450C, since DP stress–strain behavior showed a lower elastic stiffness respect to TempCore. Similar considerations can be made even for corroded conditions, with almost negligible differences respect to the reference case: this is simply explained if we consider that the main influence of corrosion is reflected on deformation parameters affecting ultimate conditions.

5 | CONCLUSIONS

The structural and economic assessment of typical residential case study buildings designed using DP and TempCore® rebars is performed, comparing results using the EAL index and accounting for two different conditions, that is, reference and corroded. Experimental data coming from a wide campaign already presented by the Authors were used for the design and to assess the deterioration level induced by aggressive environmental conditions.

Comparisons are made considering using data coming from nonlinear analyses (both pushover and IDA with selected accelerograms); the EAL index is determined using IDA results in terms of PGA activating relevant limit states, while the cost of reconstruction (%CR—the other parameter required for EAL assessment) is evaluated introducing specific modifications accounting for the increase of costs related to production process and to the different chemical composition of DP rebars. In general, IDA show average values of PGA corresponding to the yielding rotation (θ_y) lower in case of RC-B450C respect to RC-DP, while similar performance for the two case studies concerning ultimate chord rotation (θ_u) in sound condition.

In presence of corrosion, considering that the decrease of rebars' deformation due to corrosion is higher for B450C respect to DPF, the corresponding decrease of the PGA values activating relevant limit states is higher for TempCore® (26%) respect to DP (15%).

Similar values of EAL index are reached for two case studies, respectively equal to 0.45% for RC-DP and 0.52% for RC-B450C, without appreciable differences shifting from reference to corroded condition. At last, it is important to underline that the results are influenced by many factors such as the seismic input, the high mechanical performance of TempCore® rebars here presented, and the level of corrosion entity, but, as a general consideration, it is reasonable to say that the structural response between RC-DP and RC-B450C is very similar in reference condition, while the adoption of DP rebars allows to achieve better performance in presence of corrosion, without otherwise requiring a strong economic impact. The proposed DP rebars could be therefore able to replace TempCore® on the actual market (of course requiring before specific intervention to adapt industrial plant), providing higher performance under corrosion as proved by the lower EAL values compared to traditional constructions.

ACKNOWLEDGMENTS

The research was developed in the framework of the European Research project NEWREBAR *"New Dual-Phase steel reinforcing bars for enhancing capacity and durability of anti-seismic moment resisting frames"* (2015–2019), funded by the Research Fund for Coal and Steel (grant agreement no. RFSR-CT-2015-00023) of European Commission. The authors would like to thank all the partners for their active contribution.

DATA AVAILABILITY STATEMENT

The data that support the findings of this study are available from the corresponding author upon reasonable request.

ORCID

Francesca Mattei https://orcid.org/0000-0002-9126-2385

REFERENCES

1. Berto L, Caprili S, Saetta A, Salvatore W, Talledo D. Corrosion effects on the seismic response of existing rc frames designed according to different building codes. Eng Struct. 2020;216:110397.
2. Berto L, Simioni P, Saetta A. Structural risk assessment of corroding RC structures under seismic excitation. Construct Build Mater. 2012;30:803–13.
3. Fang C, Lundgren K, Chen L, Zhu C. Corrosion influence on bond in reinforced concrete. Cem Concr Res. 2004;34(11):2159–67.
4. Imperatore S, Rinaldi Z, Drago C. Degradation relationships for the mechanical properties of corroded steel rebars. Construct Build Mater. 2017;148:219–30.
5. Lavorato D, Fiorentino G, Pelle A, Rasulo A, Bergami AV, Briseghella B, et al. A corrosion model for the interpretation of cyclic behavior of reinforced concrete sections. Struct Concr. 2020;21(5):1732–46. https://doi.org/10.1002/suco.201900232
6. Meda A, Mostosi S, Rinaldi Z, Riva P. Experimental evaluation of the corrosion influence on the cyclic behaviour of RC columns. Eng Struct. 2014;76:112–23.
7. EN 1998-1:2005. Eurocode 8: design of structures for earthquake resistance—part 1: general rules, seismic actions and

rules for buildings. CEN - European Committee for Standardization. 2005.
8. Keleştemur O, Yıldız S. Effect of various dual-phase heat treatments on the corrosion behavior of reinforcing steel used in the reinforced concrete structures. Construct Build Mater. 2009;23:78–84.
9. Movahed P, Kolahgar S, Marashi SPH, Pouranvari M, Parvin N. The effect of intercritical heat treatment temperature on the tensile properties and work hardening behavior of ferrite–martensite dual phase steel sheets. Mater Sci Eng. 2009;518:1–6.
10. Sarkar P, Kumar P, Manna MK, Chakraborti PC. Microstructural influence on the electrochemical corrosion behaviour of dual-phase steels in 3.5% NaCl solution. Mater Lett. 2005;59:2488–91.
11. Sarwar M, Priestner R. Influence of ferrite-martensite microstructural morphology on tensile properties of dual-phase steel. J Mater Sci. 1996;31:2091–5.
12. Caprili S, Salvatore W. Cyclic behaviour of uncorroded and corroded steel reinforcing bars. Construct Build Mater. 2015;76:168–86.
13. EN 1992-1-1:2005. Eurocode 2 (Annex C)—Design of concrete structures - Part 1–1: General rules and rules for building. 2005.
14. EN 206-1:2006. Concrete—Part 1: Specification, performance, production and conformity. 2006.
15. Maffei B, Salvatore W, Valentini R. Dual-phase steel rebars for high-ductile r.c. structures, part 1: microstructural and mechanical characterization of steel rebars. Eng Struct. 2007;29:3323–32.
16. Salvatore W, Buratti G, Maffei B, Valentini R. Dual-phase steel rebars for high-ductile r.c. structures, part 2: rotational capacity of beams. Eng Struct. 2007;29:3333–41.
17. Caprili S, Salvatore W, Valentini R. Corroded TempCore® vs dual-phase steel reinforcing bars. Construct Build Mater. 2021a;277:122301.
18. Caprili S, Mattei F, Salvatore W, Ascanio C, Luvarà G. Industrial and techno-economic feasibility of concrete structures reinforced with DP rebars. Constr Build Mater. 2021b;283:122793.
19. Caprili S, Chellini G, Mattei F, Romis F, Salvatore W. Experimental analysis on cyclic performance of concrete columns with TempCore or dual-phase steel reinforcement. Bull Earthq Eng. 2020a;18:6761–94.
20. Caprili S, Chellini G, Mattei F, Romis F, Salvatore W. Experimental assessment of the cyclic behaviour of RC-DP beam to column joints. J Earthq Eng. 2020b;1–27. https://doi.org/10.1080/13632469.2020.1759472
21. Caprili S, Mattei F, Gigliotti R, Salvatore W. Modified cyclic steel law including bond-slip for analysis of RC structures with plain bars. Earthq Struct. 2018;14(3):187–201.
22. Caprili S, Salvatore W, Valentini R, Ascanio C, Luvarà G. Dual-phase steel reinforcing bars in uncorroded and corroded conditions. Construct Build Mater. 2019;218:162–175.
23. D.M. 17/01/2018. Norme Tecniche per le Costruzioni (Italian Technical Standard for Constructions), in Italian.
24. Mazzoni, S, McKenna, F, Scott MH & Fenves GL OpenSees command language manual. Pacific Earthquake Engineering Research (PEER) Center. 2006; 264: 137–158.
25. Mander JB, Priestley MJ, Park R. Theoretical stress–strain model for confined concrete. J Struct Eng. 1988;114(8):1804–26.
26. Braga F, Caprili S, Gigliotti R, Salvatore W. Hardening slip model for reinforcing steel bars. Earthq Struct. 2015;9(3):503–39.
27. Braga F, Gigliotti R, Laterza M, D'Amato M. Modified steel bar model incorporating bond-slip for seismic assessment of concrete structures. J Struct Eng. 2012;138(11):1342–50.
28. D'Amato M, Braga F, Gigliotti R, Kunnath S, Laterza M. Validation of a modified steel bar model incorporating bond-slip for seismic assessment of concrete structures. J Struct Eng. 2012;138(11):1351–60.
29. Vamvatsikos D, Cornell CA. Incremental dynamic analysis. Earthq Eng Struct Dyn. 2002;31:491–514.
30. Morelli F., et al. Ground motions and scaling techniques for 3D performance based seismic assessment of an industrial steel structure. Bulletin of Earthquake Engineering. 2018;16(3):1179–1208.
31. Baker JW. Conditional mean spectrum: tool for ground-motion selection. J Struct Eng. 2011;137:322–31.
32. Akkar S, Sandıkkaya MA, Şenyurt M, Azari Sisi A, Ay BÖ, Traversa P, et al. Reference database for seismic ground-motion in Europe (RESORCE). Bull Earthq Eng. 2014;12:311–39.
33. Šebenik Z, Dolšek M. Strong ground motion database. University of Ljubljana, Faculty of Civil and Geodetic Engineering, IKPIR; 2016.
34. Terrenzi M, Spacone E, Camata G. Collapse limit state definition for seismic assessment of code-conforming RC buildings. International Journal of Advanced Structural Engineering, 2018;10(3):325–337.
35. Sullivan TJ, Welch DP, Calvi GM. Simplified seismic performance assessment and implications for seismic design. Earthq Eng Eng Vib. 2014;13:95–122.
36. Italian D.M. n. 65, 07-03-2017 Italian Guidelines for Seismic Risk classification of buildings.

AUTHOR BIOGRAPHIES

Silvia Caprili, Civil Engineer, PhD, associate professor, Department of Civil and Industrial Engineering, University of Pisa, Largo Lucio Lazzarino 1, 56122 Pisa, Italy. Phone: +39 050-2218244. E-mail: silvia.caprili@ing.unipi.it.

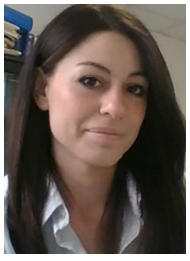

Francesca Mattei, Civil Engineer, PhD, research fellow, Department of Civil and Industrial Engineering, University of Pisa, Largo Lucio Lazzarino 1, 56122 Pisa, Italy. Phone: +39 320-9066896. E-mail: francesca.mattei@ing.unipi.it.

Walter Salvatore, Civil Engineer, PhD, full professor, Department of Civil and Industrial Engineering, University of Pisa, Largo Lucio Lazzarino 1, 56122 Pisa, Italy. Phone: +39 050-2218225. E-mail: walter@ing.unipi.it.

How to cite this article: Caprili S, Mattei F, Salvatore W. Structural and economical performance of reinforced concrete frames with Dual-Phase and TempCore® steel rebars in uncorroded and corroded conditions. Structural Concrete. 2022;23:67–80. https://doi.org/10.1002/suco.202100253